How Long Can You Make an Oxygen Chain?

Daniel J. Mckay and James S. Wright*

Contribution from the Department of Chemistry, Ottawa−Carleton Chemistry Institute, Carleton University, 1125 Colonel By Drive, Ottawa, Canada K1S 5B6

Received May 12, 1997. Revised Manuscript Received October 27, 1997

Abstract: This paper reports theoretical gas-phase structures and energetics using G2(MP2) theory for saturated oxygen chains of the general formula HO_nH. Structural trends are discussed using a simple hyperconjugation model which is capable of giving a qualitative explanation for trends in bond lengths and dihedral angles. Bond dissociation energies (BDEs) are calculated for chains of increasing length, giving 49.9, 33.9, and 17.8 kcal/mol for H_2O_2, H_2O_3, and H_2O_4, respectively. From an analysis of the radical stabilization energy of the fragments remaining after dissociation, it is shown that a minimum value for the BDE for any hydrogen polyoxide is 6.4 kcal/mol, which occurs for the center bond in H_2O_6, and that longer chains will have a higher BDE. Decomposition pathways responsible for the observed instability of the polyoxides higher than hydrogen peroxide are discussed and results are given for three low-barrier dissociation paths: a solvent-assisted path, a base-catalyzed path, and a proton relay mechanism. These mechanisms are probably general and account for the instability of polyoxide chains in proton-containing solvents. Preventing proton transfer, e.g. by perfluoroalkylation, would therefore be expected to increase chain stability, in agreement with experimental observations.

Introduction

The fact that oxygen does not form catenated chains analogous to hydrocarbon chains is one aspect which differentiates oxygen chemistry from carbon chemistry; the main other feature is its more limited capacity to form chemical bonds. The first member of the hydrogen polyoxide series, hydrogen peroxide (HO−OH), is known to have a weak O−O single bond and decomposes slowly at room temperature in aqueous solution to give water and gaseous oxygen. Higher members of the series, including hydrogen trioxide (H_2O_3) and hydrogen tetroxide (H_2O_4) are difficult to prepare and decompose in the solid state. Thus, hydrogen trioxide decomposes near −50 °C,[1−3] depending on the experimental conditions, and hydrogen tetroxide decomposes at −100 °C.[1,4] Hydrogen polyoxides containing more than four oxygen atoms have never been prepared experimentally, although the perfluorinated chains and particularly the perfluoroalkylated chains are much more stable.[5] As an example, bis(trifluoromethyl) trioxide, CF_3OOOCF_3, is stable in glass or metal at 25 °C and undergoes only slow decomposition even at 70 °C.[6]

The reason for the instability of the catenated oxygen chains has frequently been discussed in elementary texts. Thus, the very weak single-bond energies for N−N, O−O, and F−F are clearly related to the presence of strong lone pair−lone pair repulsions present in compounds such as hydrazine, hydrogen peroxide, and molecular fluorine. These repulsive effects might be expected to increase in extended chains such as the polyoxides or polynitrides, in agreement with the experimental observations on polyoxides noted above. Such repulsive effects might be expected to appear, for example, in the bond lengths in the polyoxide series, which should increase for larger chain lengths, perhaps becoming completely unbound relative to radical fragments for higher members of the series.

However, despite the widespread use and intuitive appeal of such arguments, in some aspects they are wrong. Data already exist in the literature to show that the O−O bonds in hydrogen trioxide are shorter than those in hydrogen peroxide, rather than the reverse.[7,8] More extensive data given in this paper show that these bond-shortening effects persist in all higher members of the series which were studied. Nevertheless, it is correct that the bond dissociation energy decreases for higher members of the series, finally reaching a limiting value at H_2O_6. This apparently paradoxical result has not received much discussion in the literature.

We consider the question of the conformation of an oxygen chain of arbitrary length and show it to be helical in the oxygen backbone. This observation, coupled with an analysis of the radical stabilization energy of the fragments remaining after dissociation, provides a useful way to understand the stability (or lack thereof) of the polyoxide chains. This will allow us to answer the title question, namely, "how long can you make an oxygen chain?".

This paper also studies decomposition pathways for hydrogen trioxide and hydrogen tetroxide. Our calculations show, in agreement with those by Plesničar,[9] that a solvent-assisted mechanism leads to the observed products water and singlet oxygen. We also consider other mechanisms which are expected to be general and therefore account for the observed increase in stability as the oxygen chains are perfluorinated (F_2O_n) or perfluoroalkylated ($CF_3O_nCF_3$).

(1) Giguere, P. A.; Herman, K. *Can. J. Chem.* **1970**, *48*, 3473.
(2) Plesničar, B.; Cerkovnik, J.; Koller, J.; Kovac, F. *J. Am. Chem. Soc.* **1991**, *113*, 4946.
(3) Cerkovnik, J.; Plesničar, B. *J. Am. Chem. Soc.* **1993**, *115*, 12169.
(4) Deglise, X.; Giguere, P. A. *Can. J. Chem.* **1971**, *19*, 2242.
(5) Kirchmeier, R. L.; Shreeve, J. M.; Verma, R. D. *Coord. Chem. Rev.* **1992**, *112*, 169.
(6) Anderson, L. R.; Fox, W. B. *J. Am. Chem. Soc.* **1967**, *89*, 4313.
(7) Cremer, D. *J. Chem. Phys.* **1978**, *69*, 4456.
(8) Zhao, M.; Gimarc, B. M. *J. Phys. Chem.* **1993**, *97*, 4023.
(9) Plesničar, B.; Cerkovnik, J. *J. Am. Chem. Soc.* **1996**, *118*, 2470.

S0002-7863(97)01534-5 CCC: $15.00
Published on Web 01/27/1998

Review of Theoretical Work

The literature on the chemistry of peroxides is large. *The Chemistry of Peroxides*[10] contains an article on theoretical aspects of the peroxide group by Cremer,[11] one of the authors whose work is most relevant to this paper. The more recent publication *Organic Peroxides*[12] contains an important chapter on polyoxides by Plesničar.[13] A review by Kirchmeier and co-workers covers work on the stability of fluorinated peroxides up to 1992.[5]

There have been a great many studies of hydrogen peroxide, but the theoretical study by Cremer in 1978[14] was one of the most thorough. In this paper he examined the origin of the rotational barrier using MO arguments. Earlier work of Radom, Hehre, and Pople was cited which "found a general tendency of lone pair orbitals to be coplanar with adjacent polar bonds".[15,16] An accurate study of the thermochemistry of hydrogen peroxide and other peroxides has been reported recently by Bach, Ayala, and Schlegel.[17] A study of hydrogen trioxide was also given by Cremer in a companion work to the study on hydrogen peroxide.[7] In this trioxide work he analyzed the rotational surface and in particular the origin of the global minimum for a double rotor. Jackels and Phillips[18] reported a higher level study of H_2O_3, including good estimates of errors involved in thermochemistry involving hydroxyl and hydoperoxyl radicals. Structures and energies at the SCF level were given for hydrogen trioxide more recently by Plesničar and co-workers,[2] including energetics for the hydrogen-bonded dimer $(H_2O_3)_2$. This work was notable in that it contained a detailed discussion of decomposition pathways, concluding that a cyclic dimeric structure leading to formation of $2H_2O + 2^1O_2$ was involved. Early work by Plesničar and co-workers[2,3,13] consistently invoked this type of mechanism for decomposition; although due to the difficulty of a multidimensional search for the transition state, these arguments were based on plausibility rather than on accurate calculations.

Hydrogen tetroxide was studied in detail by Fitzgerald et al.[19] It was found that the straight chain was more stable than the cyclic dimer, and they estimated that the chain structure was bound by 11 kcal/mol with respect to dissociation into hydroperoxyl radicals. They also pointed out that the central O−O bond showed a shortening of 0.12 Å relative to hydrogen peroxide (1.475 Å) and that the molecule is of C_1 symmetry, with the two longer O−O bonds being of unequal length (1.373, 1.368 Å); both of these bonds are still considerably shorter than the O−O bond in the prototype single bond in hydrogen peroxide. The question of the most stable form of H_2O_4 was reinvestigated recently by Schaefer and co-workers,[20] using extensive basis sets and correlation methods. This agreed with their earlier study and showed that a covalently bonded chain structure of C_1 symmetry lies slightly below a dimeric structure from from two HO_2 radicals in a cyclic, hydrogen-bonded geometry.

A series of calculations of strain energies in cyclic O_n molecules by Zhao and Gimarc[8] also contains data for the structures and energies of the hydrogen polyoxides H_2O_n. This study is similar in spirit to the present work, in that heats of formation are given for chains of length up to H_2O_5. However, no data were given for the radical fragments formed on dissociation, information necessary to calculate bond dissociation energies. These authors assumed that the polyoxide chains formed helical coils of C_2 symmetry and optimized structures subject to that assumption.

After this paper was completed, Plesničar and Cerkovnik[9] reexamined the question of the decomposition pathway for hydrogen trioxide and concluded that an intramolecular proton transfer mechanism with the assistance of a hydrogen-bonded solvent (water) molecule was the lowest energy path, with an activation barrier lying only 15 kcal/mol above isolated reactants (MP4 energy, MP2/6-31++G(d) geometry). As will be shown, we agree with this conclusion, subject to some qualifications associated with the energy calculated for the incipient O_2 ($^1\Delta_g$) component of the transition state.

Method of Calculation

All calculations in this paper were done with the Gaussian-94 suite of programs.[21] For reasons which will become clear in the discussion, several different levels of theory/basis sets were used. Geometry optimizations were always carried out using MP2(full) theory with a 6-31G(d) basis set. Single-point energy calculations were then carried out at these optimized geometries, corresponding to methods A, B, and C. Method A is MP2/6-311G(d,p), method B is MP2/6-311+G(3df,2p), and method C is QCISD(T)/6-311G(d,p). The complete notation for method//geometry would then be, for method A, MP2/6-311G(d,p)//MP2(full)/6-31G(d) and similarly for B and C.

Single-point energy calculations were also carried out using the G2-(MP2) method of Curtiss et al.[22] The total G2(MP2) energy at 0 K is obtained through the equation $E(\text{G2(MP2)}) = \text{QCISD(T)/6-311G(d,p)} + \text{MP2/6-311+G(3df,2p)} - \text{MP2/6-311G(d,p)} + \text{ZPE} + \text{HLC}$, where ZPE = zero-point energy and HLC = high-level correction. In terms of the energies corresponding to methods A, B, and C, above this becomes $E(\text{G2(MP2)}) = E_C + E_B - E_A + \text{ZPE} + \text{HLC}$. In the above equation, the ZPE is determined by using geometries and frequencies obtained at the HF/6-31G(d) level. These are printed without any scaling in the tables to follow, but for use in the G2(MP2) method they are scaled by a factor of 0.8929. With the inclusion of the scaled ZPE and the HLC term, this method has been shown to have an average deviation of ±1.58 kcal/mol for energetics obtained with a data set containing 55 molecules and 125 energies, including atomization energies, ionization energies, electron affinities, and proton affinities.[23] An expanded version of the G2 test set was given recently by Curtiss et al.[24] This paper also discussed the excellent results obtained with a truncated version of G2(MP2) theory entitled G2(MP2,SVP); the latter corresponds to replacing the energy term E_C by the smaller QCISD-(T)/6-31G(d) calculation (denoted E_D).

When enthalpy data are needed at 298 K, factors of $^3/_2RT$ (translation), $^3/_2RT$ (nonlinear, rotation), or RT (linear, rotation) were used. The vibrational contribution to the enthalpy from each mode of (harmonic) frequency ν_i is $E_{vib} = \Sigma_i Nh\nu_i/[\exp(h\nu_i/kT) - 1]$, plus an additional factor, RT, per species to convert from energy to enthalpy.

(10) *The Chemistry of Peroxides*; Patai, S., Ed.; Wiley: New York, 1983.
(11) Cremer, D. In *The Chemistry of Peroxides*; Patai, S., Ed.; Wiley: New York, 1983; Chapter 1.
(12) *Organic Peroxides*; Ando, W., Ed.; Wiley: New York, 1992.
(13) Plesničar, B. In *Organic Peroxides*; Ando, W., Ed.: Wiley: New York, 1992; Chapter 10.
(14) Cremer, D. *J. Chem. Phys.* **1978**, *69*, 4440.
(15) Radom, L.; Hehre, W. J.; Pople, J. A. *J. Am. Chem. Soc.* **1971**, *93*, 289.
(16) Radom, L.; Hehre, W. J.; Pople, J. A. *J. Am. Chem. Soc.* **1972**, *94*, 2371.
(17) Bach, R. D.; Ayala, P. Y.; Schlegel, H. B. *J. Am. Chem. Soc.* **1996**, *118*, 12758.
(18) Jackels, C. F.; Phillips, D. H. *J. Chem. Phys.* **1986**, *84*, 5013.
(19) Fitzgerald, G.; Lee, T. J.; Schaefer, H. F., III; Bartlett, R. J. *J. Chem. Phys.* **1985**, *83*, 6275.
(20) Fermann, J. T.; Hoffman, B. C.; Tschumper, G. S.; Schaefer, H. F., III *J. Chem. Phys.* **1997**, *106*, 5102.
(21) Gaussian-94, Revision B.3; Frisch, M. J., et al.; Gaussian, Inc., Pittsburgh, PA, 1995.
(22) Curtiss, L. A.; Raghavachari, K.; Trucks, G. W.; Pople, J. A. *J. Chem. Phys.* **1993**, *98*, 1293.
(23) Curtiss, L. A.; Raghavachari, K.; Trucks, G. W.; Pople, J. A. *J. Chem. Phys.* **1993**, *98*, 1293.
(24) Curtiss, L. A.; Raghavachari, K.; Redfern, P. C.; Pople, J. A. *J. Chem. Phys.* **1997**, *106*, 1063.

Table 1. Bond Lengths (in Å) in the Hydrogen Polyoxides H_2O_n and Related Radical Fragments HO_n Using MP2(full)/6-31G(d) Theory[a]

species	H−O_1	O_1−O_2	O_2−O_3	O_3−O_4	O_4−O_5	O_n−H	method	ref
H_2O	0.9686					0.9686		
	0.9575					0.9575	exptl	*b*
H_2O_2	0.9756	1.4681				0.9756		
	0.968[e]	1.475					exptl	*b*
H_2O_3	0.9798	1.4412	1.4412			0.9798		
	0.980	1.442	1.442			0.980	MP2/DZP	7
H_2O_4	0.9801	1.4480	1.4296	1.4353		0.9813		
	9.950	1.373	1.356	1.368		0.950	HF/DZP	19
	0.9719	1.4342	1.4353	1.4342		0.9719	MP2/6-31G(d,p)	8
H_2O_5	0.9804	1.4372	1.4394	1.4315	1.4336	0.9808		
	0.9720	1.4344	1.4334	1.4334	1.4344	0.9720	MP2/6-31G(d,p)	8
HO	0.9790							
	0.9699						exptl	*b*
$HO_2(^2A'')$	0.9832	1.3251						
	0.971	1.330					exptl	*c*
$HO_2(^2A')$	0.9813	1.3957						
HO_3	0.9860	1.4431	1.2624					
HO_4	0.9806	1.4249	1.4354	1.2845				
O_2 ($^3\Sigma_g^-$)		1.2460						
		1.2075					exptl	*d*
O_2 ($^1\Delta_g$)		1.2738						
		1.2156					exptl	*d*

[a] Structures are drawn and atoms are labeled in the text. [b] *CRC Handbook of Chemistry and Physics*, 75th ed.; Lide, D. R., Ed.; CRC Press: Boca Raton, FL, 1995. [c] Lubic, K. G.; Amano, T.; Vehara, H.; Kawaguchi, K.; Hirota, E. *J. Chem. Phys.* **1984**, *81*, 4826. [d] Reference 20. [e] Recommended value in ref 14.

Since bond dissociation energies are the focus of this paper, the above formulas were only used to convert experimental enthalpies of formation at 298 K to bond dissociation energies at 0 K for purposes of comparison.

Molecular structures are reported using the MP2(full)/6-31G(d) level of theory. Many of these structures have been reported in the literature previously with a variety of methods; however, to establish our arguments it is important to have a consistent set of values.

Results and Discussion

Structures of Hydrogen Polyoxides H_2O_n. Optimized molecular structures are shown for hydrogen peroxide (**1**), hydrogen trioxide (**2**), hydrogen tetroxide (**3**) and hydrogen pentoxide (**4**) and for the radicals HO_3 (**5**) and HO_4 (**6**). The corresponding bond lengths for these structures and related molecules are found in Table 1, bond angles in Table 2, and dihedral angles in Table 3.

Variations in bond lengths have been discussed on a molecule-by-molecule basis, e.g., by Cremer for H_2O_2[14] and H_2O_3[7] and by Schaefer and co-workers[19,20] for H_2O_4. Here, we are interested in the general trends. For the bond lengths, Table 1 shows that the MP2 O−H bond lengths are too long by ca. 0.01 Å, where the results are accurately known (H_2O and H_2O_2). We assume that this result holds for the higher polyoxides, allowing a useful MP2 comparison of trends as the chain lengthens. From the table is it clear that the O−H bond shows a slight lengthening on going from H_2O to H_2O_2. However, a smaller bond lengthening continues for the higher polyoxides, and we estimate that an asymptotic value would be reached at 0.981 Å (MP2), corresponding to an experimental value of ca. 0.971 Å.

The O−O bond lengths, on the other hand, are underestimated by ca. 0.01 Å at the MP2/6-31G(d) level. There is a large bond shortening of 0.027 Å on extending the chain to H_2O_3. There is a further significant shortening of 0.012 Å on going to the shortest, central bond in H_2O_4, although by much less than the amount predicted by Fitzgerald et al. using an RHF method.[19] Finally, at H_2O_5 the bond lengths begin to increase again, although the shortest bond is only 0.0002 Å longer than in H_2O_4. Notice that in H_2O_5 *all* of the O−O bond lengths are shorter than in H_2O_2, and by a substantial amount (not less than 0.028 Å). Clearly, the simple idea that the increase in lone pair repulsions with increasing chain length should cause an increase in O−O bond distance is incorrect, and a more sophisticated analysis is needed.

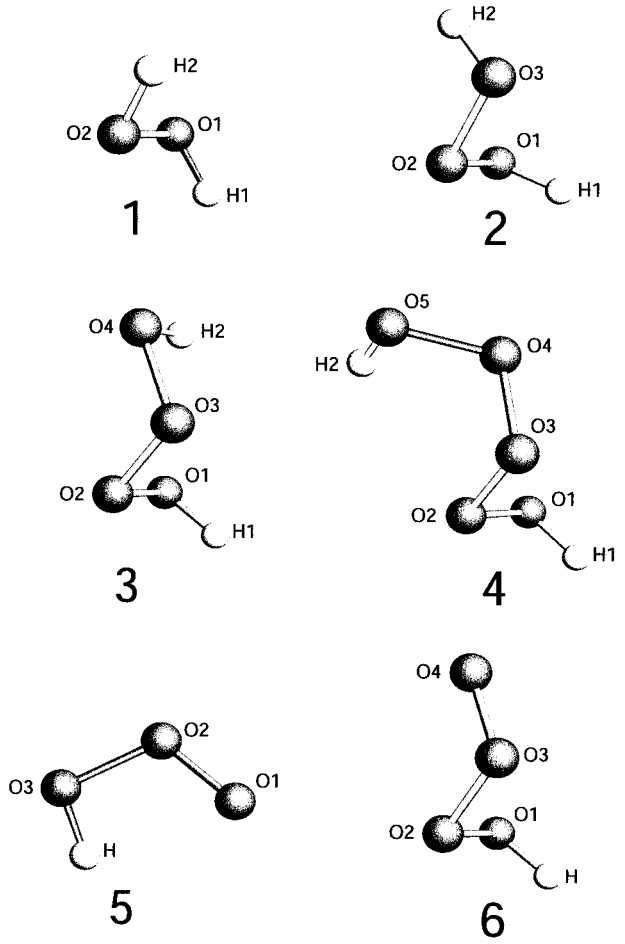

Table 2. Bond Angles (in degrees) in the Hydrogen Polyoxides and Related Radical Fragments

species	H−O$_1$−O$_2$	O$_1$−O$_2$−O$_3$	O$_2$−O$_3$−O$_4$	O$_3$−O$_4$−O$_5$	O−O−H
H_2O_2	98.7				98.7
theor	98.7				98.
exptl ref	98.5 ± 1				98.5 ± 1
H_2O_3	100.3	106.2			100.3
theor ref	100.3	106.1			100.3
H_2O_4	100.3	105.3	106.5		99.9
theor ref	103.8	107.1	107.9		103.8
H_2O_5	100.6	107.0	106.2	106.6	100.1
$HO_2(^2A'')$	104.5				
theor ref	104				
HO_2 ($^2A'$)	101.2				
HO_3 ($^2A''$)	98.9	111.1			
HO_4	101.0	105.7	110.0		

Table 3. Dihedral Angles (in degrees) in the Hydrogen Polyoxides and Related Radical Fragments Using MP2(Full)/6-31G(d) Theory

species	H−O$_1$−O$_2$−O$_3$	O$_1$−O$_2$−O$_3$−O$_4$	O$_2$−O$_3$−O$_4$−O$_5$	O−O−O−H	method	ref
H_2O_2	121.2					
	119.8				exptl	*a*
	119.4				MP2/DZP	14
H_2O_3	78.1			−78.1		
	78.5			−78.5	MP2/DZP	7
H_2O_4	83.8	−77.3		77.5		
	81.6	−78.5		81.6	MP2/6-31G(d,p)	8
H_2O_5	81.2	−75.4	−75.9	85.7		
	84.6	−79.9	−79.9	84.6	MP2/6-31G(d,p)	8
HO_3	0.0					
HO_4	88.0	−75.5				

[a] Reference *b*, Table 1.

For the multiply bonded oxygen molecules, i.e., O_2 ($^3\Sigma_g^-$) and O_2 ($^1\Delta_g$), the MP2 bond lengths are very poor, giving errors of ca. 0.04 and 0.06 Å, respectively. This is large but typical for multiply bonded systems, as shown in a paper on the performance of G2 theory by Curtiss et al.[25] Since decomposition pathways described later involve formation of singlet oxygen, this rather large error in geometry signals that care is required in interpretation of activation barriers where singlet oxygen is formed.

Bond angles (Table 2) are well described at this level, giving essentially exact agreement with experiment for H_2O_2 and good agreement with the calculated literature values.[8,14] These are less important for the arguments to follow and, for that reason, will only be discussed further in context.

The dihedral angles, on the other hand, are very important for determining accurate conformations of the polyoxides. Table 3 shows that the calculated (HOOH) dihedral angle for H_2O_2 is within 2° of the experimental value. The dihedral angle which involves the end hydrogen drops drastically from 120° in H_2O_2 to ±78° in H_2O_3. For H_2O_4 and the higher polyoxides, the average value of the dihedral angles containing the two terminal H atoms is slightly greater than 80°. Note that the optimized structures are somewhat asymmetric in the HOOO dihedral angles at either end of the chain; thus, deviations from C_2 symmetry up to 6° occur for H_2O_4.

Comparing to other theoretical values, good agreement is obtained with calculated values of Cremer[7] (H_2O_3) and Zhao and Gimarc[8] (H_2O_4 and H_2O_5), although the latter authors assumed C_2 symmetry for H_2O_4 and H_2O_5. In fact, when the polyoxides are optimized without any symmetry constraint, only H_2O_3 has C_2 symmetry, whereas H_2O_4 and H_2O_5 do not. As discussed by Fitzgerald et al.[19] for H_2O_4, the C_2 symmetry is broken by the asymmetry of the hydrogen atoms. Their orientation is actually determined by hyperconjugation, rather than hydrogen bonding as suggested by Fitzgerald et al.[19] (see discussion below). However, an approximate C_2 symmetry is maintained for the oxygen backbone, even in H_2O_4 and H_2O_5.

As shown in structures **3** and **4** and in Table 3, the O−O−O−O dihedral angle stays approximately constant at 76.4 ± 1° as the chain length is increased. This is also true in the radical HO_4. The result is that whenever there are four or more oxygens present in the parent molecule H_2O_n a tight helical coil is formed, and this helical shape is preserved even in the radical fragments HO_n. This tendency toward helix formation along the series was first pointed out by Zhao and Gimarc,[8] to the best of our knowledge. The beginnings of the helical turn appear even in H_2O_3 (structure **2**), and it can be seen from a comparison of structures **2**−**4** that the conformation of the oxygen backbone of H_2O_n is preserved on extending the chain to H_2O_{n+1}. The origin of this remarkable behavior, as well as the trends in O−H and O−O bond lengths, has to lie in the inherent tendency of the oxygen chain to assume a skew geometry with a regular twist on addition of each new oxygen atom. The torsional potentials have been discussed in the literature at some length, particularly for H_2O_2 [ref 14 and references cited therein] and to a lesser extent for H_2O_3.[7] Here we attempt to provide a simple and clear-cut analysis which is nevertheless capable of explaining all of the above trends, including the changes in O−O bond lengths and dihedral angles. First, it is necessary to review the behavior of the HOOH and HOOF torsional potentials.

The optimized (i.e., fully relaxed) RHF/6-31G(d,p) torsional potential for HOOH reaches a minimum near a dihedral angle of 121° (skew geometry), with maxima of 0.87 kcal/mol for the trans (180°) and 8.60 kcal/mol for the cis (0°) barrier height. This is close to the best values obtained by Cremer[14] using an MP2/DZP calculation (skew 0.00, trans 0.60, cis 8.79 kcal/mol), i.e., the barrier shape is relatively unaffected by the MP2 correlation contribution. The FOOH torsional potential is quite

(25) Curtiss, L. A.; Raghavachari, K.; Pople, J. A. *J. Chem. Phys.* **1995**, *103*, 4192.

different, with a minimum at 83° (skew), a very high trans barrier lying 7.08 kcal/mol above the minimum and a similar cis barrier of 6.73 kcal/mol. This is in reasonable agreement with a recent study.[26]

Hyperconjugation plays a dominant role in determining the optimum dihedral angles. To see this, consider the composition of localized (σ, σ^*) on O−H and O−O. Valence orbital ionization energies are −13.6 eV for the 1s orbital on H and −20 eV for an sp^3 orbital on oxygen. Hybridization on F can be considered to lie between −19.0 eV (unhybrizided p orbital on F) and −24 eV (sp^3 orbital on F), i.e., a mean value of ca. −22 eV. The σ_{OH} bonding orbital therefore contains much more $sp^3{}_O$, whereas the σ^*_{OH} antibonding orbital contains much more $1s_H$. The trans configuration minimizes lone pair repulsions (or bond−dipole repulsions), and on this basis alone, the dihedral angle τ is expected to be 180°. However, hyperconjugation, which amounts to mixing σ^*_{OH} with a lone pair on the adjacent oxygen is optimum when τ is 120°. This is the case because the σ^*_{OH} is largely centered on the H atom, so that hyperconjugation is optimum when H lines up with the opposite lone pair, which occurs at 120°. Clearly, hyperconjugation is the dominant effect, since the latter corresponds to the observed dihedral angle. However, the stability of the trans structure results in their being only a small difference in energy (<1 kcal/mol) between trans and skew conformations.

In FOOH, the OF bond is fairly nonpolar, since it is mixing two components of nearly equal energy. Now σ_{OF}* has a significant component on oxygen. This results in maximum stabilization when lined up with a lone pair on the adjacent oxygen, which occurs at $\tau = 60°$. At the same time, the interaction of σ^*_{OH} described above is optimum at $\tau = 120°$. The lone pair−σ_{OF}* interaction is expected to be dominant over the lone pair−σ^*_{OH} interaction due to better spatial overlap (σ^*_{OH} is centered near H, whereas σ_{OF} is centered near O). The molecule splits the difference, locating its optimum position somewhat closer to 60 than to 120° (83.4° in our calculation).[26]

The torsional potential in FOOF has a minimum in the skew geometry at 87.5°.[27,28] Reproducing this potential curve, as well as bond distances in FOOF, has proven to be particularly difficult for ab initio calculations. MP2 values are reasonable, but quite sensitive to the quality of the basis set used.[28] Clearly, the position of the minimum is close to that in FOOH, proving that this system more closely resembles the extended polyoxide torsional angles than it does HOOH.

Next consider torsional angles in H_2O_3 (structure **2**). In H−O1−O2−O3, suppose that the HOOO dihedral angle was set to $\tau = 0°$ (cis configuration of H−O−O−O, see structure **5**). Denote the lone pairs on O1, O2, and O3 as (n_{1a}, n_{1b}), (n_{2a}, n_{2b}), (n_{3a}, n_{3b}), respectively. The cis conformation is a maximum since lone pair repulsions are maximized. Rotation of the OH group about the O1−O2 bond to $\tau = +60°$ (i.e., when viewed along the O1−O2 axis, lying above the O−O−O plane) optimally lines up σ^*_{O2O3} with n_{1b}. Further rotation to $\tau = 120°$ lines up σ^*_{OH} (centered on H) with n_{2a}. Our case is now analogous to FOOH, and the dihedral angle is predicted to be +90° (MP2 calcd +78°). Now consider the other end of the molecule, in particular the dihedral angle H2−O3−O2−O1. The atom H2 cannot lie on the same side of the plane as atom H1, because then lone pair n_{2a} has already been used for hyperconjugation. Instead, the (unused) lone pair n_{2b} lines up with H2, forcing the dihedral angle to be −60°. In addition σ^*_{O1O2} lines up with n_{3b} causing the angle to be −120°. As before, an angle slightly below −90° results (MP2 calcd −78°). In fact, the molecule when optimized has true C_2 symmetry so that both HOOO dihedral angles are necessarily equal and opposite.

It remains to explain the shortening of the OO bond on extension of the chain. In hydrogen peroxide, which serves as the reference standard of O−O bond length = 1.468 Å (MP2), hyperconjugation arising from the two lone pair−σ^*_{OH} interactions helps to establish the O−O bond length. These hyperconjugative effects are relatively weak, as described above, relative to those arising from lone pair−σ^*_{OO} interactions in the larger chains. In H_2O_3, for example, the O1−O2 bond is shortened by hyperconjugation from lone pair−σ^*_{OH} (weak) and simultaneously from lone pair−σ^*_{O2O3} (strong). The result is a significant bond shortening relative to the OO bond in HOOH, so that we observe a change (MP2) from 1.468 to 1.441 Å. Because of the very small changes in OH bond lengths, we omit any discussion of their variations.

Now consider the extension of the above ideas to predict the geometry of H_2O_4. First, it is obvious that the central bond O2−O3 will be shortened by hyperconjugation from two adjacent lone pair−σ^*_{OO} interactions, which would include O1−O2 and O3−O4. Since the bonds O1−O2 and O3−O4 each have one hyperconjugative interaction from σ^*_{OH}, the central bond is expected to be shortest. Table 1 shows that this is indeed the case, the central O−O bond being the shorter of the three (1.4296 Å vs 1.4480 and 1.4353 Å).

Dihedral angles in H_2O_4 are established as follows. H1−O1−O2−O3 is the same as described above for H_2O_3 and for the same reasons. O4 now adopts a geometry formerly occupied by the terminal hydrogen H2 in H_2O_3, for similar reasons. The only angle remaining to establish is the terminal dihedral angle O2−O3−O4−H2. When all lone pair−σ^*_{OO} interactions are used once and only once, the only remaining stabilizing interaction is H2-n_{3b}. This rotates the terminal H2 below the plane of O2−O3−O4 and also destroys the C_2 symmetry in the process. The molecule appears to have an internal hydrogen bond between O1−H2−O4, as stated by Fitzgerald et al.,[19] but if this were true the bond would be highly bent (angle O1−H2−O4 = 100° and also rather long ($R_{O\cdots H}$ = 2.47 Å). From the discussion above it can be seen that it is not necessary to invoke internal hydrogen bonding; all torsional angles can be explained by a strict accounting for all hyperconjugative interactions and using each such interaction once and only once.[29] This approach leads to the beginnings of a helix coil in H_2O_4, although with broken symmetry.

H_2O_5 (structure **4**) continues the helical turn. This structure can also be predicted by the arguments given above. By extension, an infinite chain will form a tightly coiled helix, with a dihedral angle of 78° as each new oxygen atom is added.

Structures of Radicals HO_n. Structures of the HO and HO_2 radicals are known experimentally[30,31] and will not be discussed at length here, except to point out that the hydroperoxyl radical exists in two electronic states, the lower of which is the π radical of $^2A''$ symmetry. Thus, care is needed with these calculations to be sure that the correct electronic state is being studied. The difference in O−O bond lengths in the two states is substantial,

(26) Francisco, J. S. *J. Chem. Phys.* **1993**, *98*, 2198.

(27) Harmony, M. D.; Laurier, V. W.; Kuczkowski, R. L.; Schwendeman, R. H.; Ramsay, D. A.; Lovas, F. J.; Lafferty, W. J.; Maki, A. G. *J. Phys. Chem. Ref. Data* **1979**, *8*, 619.

(28) Lee, T. J.; Rice, J. E.; Dateo, C. E. *Mol. Phys.* **1996**, *89*, 1359.

(29) Interactions between σ^* orbitals and lone pairs are only stabilizing when each interaction occurs once only.

(30) Huber, K. P.; Herzberg, G. *Molecular spectra and Molecular Structure. IV. Constants of Diatomic Molecules*; Van Nostrand: New York, 1979.

(31) Johns, J. W. C.; McKellar, A. R. W.; Riggin, M. *J. Chem. Phys.* **1978**, *68*, 3957.

Table 4. Zero-Point Energy and Total Energy (in hartree) for the Hydrogen Polyoxides and Related Radicals[a]

species	ZPE[b]	E_A	E_B	E_C	E(G2(MP2))
H(^{2}S)	0.00000	−0.49981	−0.49981	−0.49981	−0.50000
O(^{3}P)	0.00000	−74.91814	−74.95242	−74.93402	−74.97868
$O_2(^3\Sigma_g^-)$	0.00460	−150.02336	−150.10731	−150.03681	−150.14202
$O_2(^1\Delta_g)$	0.00455	−149.97390	−150.06037	−149.98719	−150.09959
HO($^2\Pi$)	0.00914	−75.57275	−75.61741	−75.58921	−75.64089
H_2O	0.02297	−76.26365	−76.31811	−76.27607	−76.33001
$HO_2(^2A'')$	0.01571	−150.58524	−150.67664	−150.61519	−150.72275
$HO_2(^2A')$	0.01511	−150.55350	−150.64414	−150.58302	−150.69036
$HO_3(^2A'')$	0.02030	−225.57633	−225.71673	−225.62095	−225.78841
HO_4	0.02485	−300.55639	−300.74432	−300.61175	−300.83769
H_2O_2	0.02930	−151.23085	−151.32863	−151.25470	−151.36132
H_2O_3	0.03420	−226.21849	−226.36317	−226.25354	−226.41769
H_2O_4	0.03865	−301.20400	−301.39676	−301.25061	−301.47387
H_2O_5	0.04281	−376.18886	NC[c]	−376.24688	NC

[a] For definitions of E_A, etc., see text. [b] ZPE = unscaled zero-point energy from HF/6-31G(d) calculation; G2 energies contain scaled ZPE (see text). [c] NC = not calculated due to excessive memory and/or CPU time required.

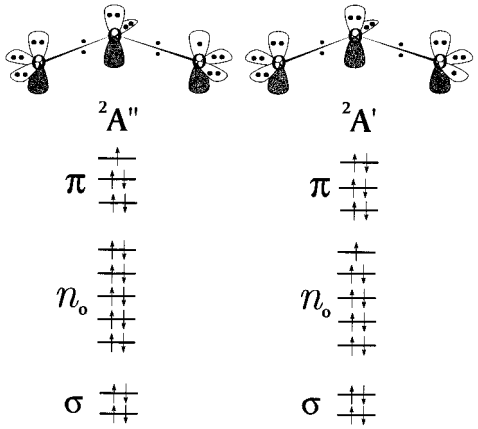

Figure 1. Comparison of MO diagrams showing the stability of the O_3^- radical in π ($^2A''$) vs σ ($^2A'$) orbitals.

and the ground electronic state has begun to acquire some π character resembling diatomic oxygen, hence its very short (MP2) bond length of 1.325 Å.

The HO_3 radical has one O−O bond typical of the polyoxides (1.4431 Å), but another which is very short (1.2624 Å) and close to the bond length in ozone (exptl 1.272 Å[32]). Unlike its neutral parent H_2O_3, with HOOO dihedral angles of 78°, the HO_3 radical is planar with dihedral angle $\tau = 0.0°$. Comparison of Tables 1 and 3 and structures **3** and **6**, however, shows that H_2O_4 and HO_4 have essentially identical geometries in terms of torsional angles. This is also true in the radical for the bonds O1−O2 and O2−O3 which are close to those in the parent; however, O3−O4 also shows a short bond length comparable to ozone.

A good analogy for the terminal OOO radical, as in HO_3, is the ozonide ion O_3^-, since the H atom similarly contributes an extra electron to O_3. On the basis of MOs appropriate to O_3^-, an explanation for why the π radical is preferred can be seen in Figure 1. If C_s symmetry is assumed, the π radical is $^2A''$ and the σ radical is $^2A'$. An MO diagram (Figure 1) shows that the manifold of π, nonbonding (n), and σ MOs creates the two electronic states shown in the figure. Here, the lowest π MO is bonding, the middle is nonbonding, and the top (3π) is antibonding. Since there are five electrons in the π system ($^2A''$) vs six in $^2A'$, and since the lone pair orbitals will definitely lie below 3π, it is obvious that the most stable radical must correspond to partial occupation of 3π. The total π bond order is 0.5, spread over 2 bonds, giving a total bond order ($\sigma + \pi$) of 1.25. The bonds will shorten somewhat, probably in an asymmetric way when an H-atom replaces the extra electron. This agrees with Table 1 for the HO_3 structure.

For HO_4 and higher radicals, the HO end of the molecule begins its helical turn (structure **6**), so the terminal OOO end is removed from strong interaction with the rest of the molecule. The same arguments apply, then, that the π form of the radical is preferred over the σ form.

Thermochemistry. In this section, we examine the bond dissociation energy for H_2O_n and HO_n. To allow extrapolation to the general polyoxide H_2O_n, total (electronic) energies, zero-point energies, and atomization energies are required in order to derive average bond energies. The average bond energies are used to obtain radical stabilization energies (RSEs). The RSEs are then used to create an additivity scheme which not only correlates well with the calculated G2(MP2) energies but also allows us to discuss the stability of a chain of arbitrary length.

Table 4 shows the calculated zero-point energy and the total energy, obtained according to the four methods described earlier, for the relevant radical fragments and neutral hydrogen polyoxides. In the last column, the G2(MP2) energy already contains the scaled zero-point energy; the other columns (E_A, E_B, E_C) do not. The G2(MP2) energy therefore corresponds to the internal energy E_0 at 0 K (in the notation of Curtiss et al.,[23] this is referred to as $\sum D_0$.)

As shown in Table 4 from the G2(MP2) energy, the $^2A''$ state of HO_2, which is the π radical, lies 20.3 kcal/mol below the $^2A'$ form, which is the σ radical. This is in reasonable agreement with other calculations in the literature.[33] The HO_3 radical presents an interesting case. At the ROHF/6-31G(d) level, where the ZPE correction is determined, the σ radical is the lowest energy state. The radical has an HOOO dihedral angle of ca. 90°. This is similar to an H_2O_3 molecule (structure **2**) which has had one O−H bond truncated. At the MP2(full) level using the same basis set, however, the radical becomes planar ($\tau = 0$) so that the $^2A''$ state is lowest. This corresponds to structure **5**. For HO_4 and higher radicals, the terminal oxygen could always be present as a σ or a π radical. In general, the π radical will be more stable, for reasons described previously.

Table 5 shows the atomization energy at 0 K for A, B, C, and G2(MP2), denoted $\Delta E°_0$. These data are plotted in Figure 2. Data from which atomization energies were derived (Table 4) were complete for methods A and C, giving rise to the two plots extending from 2 to 5 oxygen atoms in the figure. These data are highly linear, with small least-squares deviations in

(32) Barbe, A.; Secroun, C.; Jouve, P. *J. Mol. Spectrosc.* **1974**, *49*, 171.

(33) Varandas, A. J. C.; Voronin, A. I. *J. Phys. Chem.* **1995**, *99*, 15846.

Table 5. Atomization Energy $\Delta E_0°$ at 0 K (in kcal/mol) for Hydrogen Polyoxides and Related Radical and Decomposition Fragments[a]

species	A	B	C	G2(MP2)
$O_2(^3\Sigma_g^-)$	114.81	124.47	103.32	115.88
$O_2(^1\Delta_g)$	83.80	95.04	72.22	89.25
HOH	204.17	216.84	202.00	220.46
$OH(^2\Pi)$	92.02	98.53	92.38	101.90
$HO_2(^2A'')$	147.53	161.87	146.40	166.66
$HO_3(^2A'')$	190.73	214.31	188.85	220.95
HO_4	227.04	258.93	221.93	265.42
H_2O_2	231.41	249.76	226.45	253.73
H_2O_3	272.28	298.54	264.38	302.48
H_2O_4	312.05	346.98	301.45	351.12
H_2O_5	351.58	395.6 ± 0.8[b]	338.18	399.8 ± 0.3[b]
slope[c]	40.03 ± 0.22	48.61 ± 0.10	37.23 ± 0.19	48.69 ± 0.03
intercept[c]	151.7 ± 0.8	152.6 ± 0.3	152.3 ± 0.7	156.4 ± 0.1

[a] Method A, B, and C (see text for definition) now use HF ZPEs (Table 4) scaled by 0.8929 for the molecule or radical; same for G2(MP2). [b] Extrapolated value from a least-squares fit to plot of atomization energy vs number of oxygen atoms, see Figure 3. [c] Least-squares slope and intercept from fit to data in Figure 3.

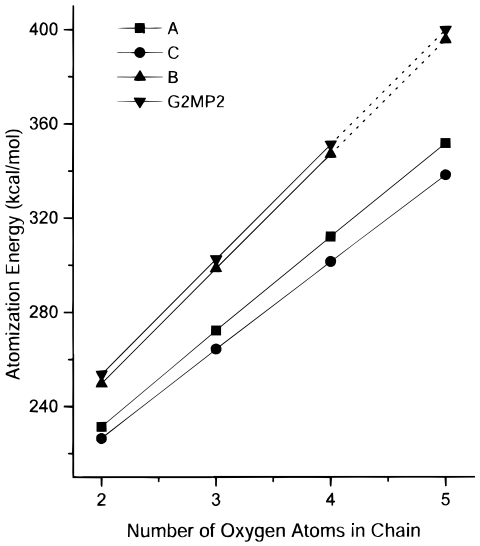

Figure 2. Atomization energy $\Delta E_0°$ vs number of oxygen atoms in the hydrogen polyoxide chains H_2O_n.

the slope included in Table 5. This implies that the O−O bonds are essentially identical and independent of the number of oxygen atoms in the chain. This is true because the only change in bonding (hence atomization energy) from H_2O_n to H_2O_{n+1} is the addition of one more O−O bond.

Data in Table 4 for methods B and G2(MP2) only extend over 2−4 oxygen atoms, but assuming linearity we can then extrapolate to obtain a G2(MP2) energy for H_2O_5. This can be done either by extrapolating B and then adding the high-level correction (HLC) to obtain the G2(MP2) energy, or simply by extrapolating the G2(MP2) energy from the three data points shown; both agree well, but the latter method was used. The extrapolation introduces an uncertainty of 0.3 kcal/mol into the computed G2(MP2) atomization energy for H_2O_5, as shown in Table 5. Note that we are now able to obtain an atomization energy for a chain of arbitrary length, assuming only that this extrapolation procedure is valid.

The G2(MP2) slope (Figure 2, see also Table 5) is 48.69 ± 0.03 kcal/mol. This corresponds to the average bond energy (ABE) of an O−O bond, because it represents the incremental energy obtained on adding an oxygen atom to the growing polyoxide chain. The only way that the slope could be constant

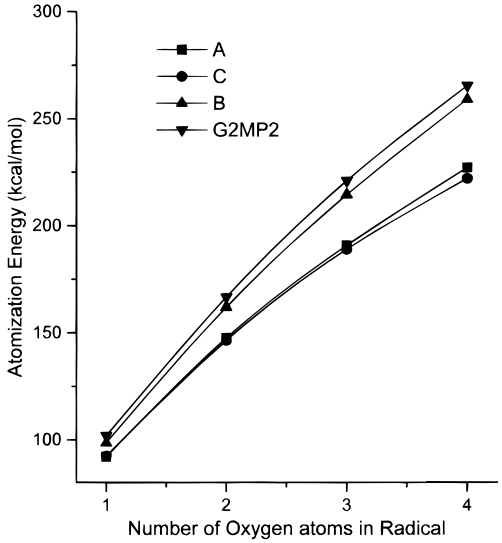

Figure 3. Atomization energy $\Delta E_0°$ vs number of oxygen atoms in the hydrogen polyoxide radical chains HO_n.

is if the two terminal OH bonds also have a constant ABE as the chain grows longer. This will occur as an oxygen atom is added if, in order of decreasing importance, (i) the bond distance of the O−H bond stays constant, (ii) the terminal HOO bond angle stays constant, and (iii) the terminal HOOO dihedral angle stays constant, where these statements all refer to the hydrogen polyoxide H_2O_n. Use of our G2(MP2) results from Tables 1−3 shows that, on going from H_2O_2 to H_2O_5, (i) the O−H bond lengths do not change by more than 0.005 Å, (ii) the HOO bond angles do not change by more than 2°, and (iii) the HOOO dihedral angles do not change by more than 2°. These conditions satisfy the most obvious requirements for a constant OH average bond energy.

A less obvious requirement is that the atomic charges in the OH bond should remain approximately constant as the chain is enlarged. A Mulliken population analysis of the atomic charge on H in H_2O_2, H_2O_3, H_2O_4, and H_2O_5 showed values ranging from +0.47e to +0.46e, respectively; therefore, so this condition is also satisfied.

Given that the average bond energy of an O−O bond is 48.69 kcal/mol, as derived above, the average bond energy of an O−H bond can be obtained as follows: For HOOH → 2H + 2O, the atomization energy (Table 5) = ABE(O−O) + 2ABE(O−H), so that ABE(O−H) = 102.52 kcal/mol. Continuing for H_2O_n, the atomization energy (Table 5) = $(n - 1)(48.69)$ + 2ABE-(O−H). This gives 102.52, 102.55, 102.53, and 102.52 kcal/mol for n = 2, 3, 4, and 5, respectively, for a best value of ABE(OH) = 102.53 ± 0.02 kcal/mol for the series.

The same type of analysis can be used for the radicals HO_n. Using data from Table 5, the atomization energy (at 0 K) is plotted for the radicals HO, HO_2, HO_3, and HO_4 in Figure 3. With all methods, the atomization energy varies in a distinctly nonlinear way with respect to increasing the length of the radical. Why should this be so different from the result obtained with the parent hydrogen polyoxides?

Recall from Table 1 that while the OH bond lengths are constant to within 0.007 Å for the HO_n radicals above, there are drastic variations in the O−O bond lengths. In the cases including HO_2, HO_3, and HO_4, the terminal O−O bond is short (1.26−1.33 Å) whereas the other bonds are long (1.43 ± 0.01 Å). The radicals therefore contain essentially one partial double bond (actually closer to the bond order of 1.5 as in ozone) and $n - 2$ single bonds. The average bond energy in ozone is 72

Table 6. Radical Stabilization Energy (RSE) for HO_n Radicals (in kcal/mol)

species	RSE
HO	−0.61
HO_2	15.42 ± 0.03
HO_3	21.16 ± 0.20
HO_4	16.60 ± 0.20

kcal/mol.[34,35] Using the intervals between HO and HO_2, HO_2 and HO_3, etc., from Table 5 (i.e., the changing slopes in Figure 2), we obtain incremental O−O ABEs of 65, 54, and 45 kcal/mol, respectively. This indeed shows a variation between the ozone-like bond energy in HO_2 and is close to (actually somewhat less than) the O−O single bond energy for the longer chain HO−O−O−O.

A useful way to interpret the above results is in terms of the radical stabilization energy (RSE).[36,37] As an O−H bond in H_2O_2 is broken, for example, the HO_2 radical is stabilized, undergoing a significant geometry relaxation relative to the parent HO−OH. This RSE could be quantified, for example, by comparing the energy difference between HO_2 in its true (relaxed) geometry with that of HO_2 taken at the geometry present in H_2O_2. A disadvantage of the above definition, however, is that it does not allow a method to calculate zero-point energy for the unrelaxed radical, since it does not lie at a potential minimum.

Another way to define RSE which avoids this problem is to set the RSE of the HO radical to be zero by definition. A better fit to G2(MP2) bond dissociation energy data will result, however, if the HO radical is itself assigned an RSE. To accomplish this, we take the ABE from the hydrogen polyoxides derived previously (48.69 kcal/mol for O−O) and obtain BDE(HO−OH) using data from Table 5; then BDE(HO−OH) = ABE(O−O) − 2RSE(HO), or 49.91 = 48.69 − 2RSE(HO), so that RSE(HO) = −0.61 kcal/mol.

RSEs for the other radicals HO_2, HO_3, and HO_4 are derived as follows: For HO_2, we use the two reactions HO_2−OH → HO_2 + HO, and HO_2−O_2H → 2HO_2. The former gives BDE(HO_2−OH) = ABE(O−O) − RSE(HO_2) − RSE(HO) = 15.39 kcal/mol, obtaining BDE data from the G2(MP2) atomization energies. The latter reaction gives 15.45 kcal/mol, so that an average value of RSE(HO_2) = 15.42 kcal/mol. The two relevant reactions creating HO_3 radicals are HO_3−OH → HO_3 + HO and HO_3−O_2H → HO_3 + HO_2, giving 21.34 and 20.97 kcal/mol, for an average value of 21.16. Continuing in the same way for HO_4, we obtain the values of RSE listed in Table 6.

The radicals HO_2, HO_3 and HO_4 all show substantial RSEs. This can again be understood by considering the degree of π stabilization in the various radicals. Thus, HO_2 (structure not shown) is planar with a π system as in O_2, and has an RSE of 15.4 kcal/mol. HO_3 (**5**) is also planar with the O−O−O unit showing an ozone-like stabilization in the π system and a maximum RSE of 21.2 kcal/mol. For larger radicals, the RSE will be less, e.g., as in HO_4 (**6**) where the RSE is 16.6 kcal/mol. Inspection of structure **6** reveals why. HO_4 is nonplanar and has begun the helical coiling caused by hyperconjugative stabilization which is characteristic of the parent polyoxides. Now the remaining RSE comes mostly from the π system on the two terminal oxygens (O4 and O3) which are connected by the short bond of 1.28 Å. The long O2−O3 bond does not contribute significantly to the RSE since O2 is bonded to O1 with a dihedral angle of 75° (beginning of the helical coil). This same result is expected for any larger radical, e.g., HO_5, HO_6, and higher, all of which will have RSE values near 16 kcal/mol since the radicals will be helical with stabilization occurring only on the terminal two oxygen atoms. The HO_3 radical is therefore most stabilized of all of the possible radicals. Because of the regularity in O−O bond energy in the hydrogen polyoxides and since the nature of the radical fragments determines the RSE, we can predict that the smallest bond dissociation energy for any hydrogen polyoxide will occur for the decomposition H_2O_6 → 2HO_3. As the chain length is increased, a constant value around 16 kcal/mol will be reached for large radical fragments, so that a limiting value of the minimum BDE for long chains will be ca. 48−2(16) = 16 kcal/mol if the chain is broken in the middle. If the long chain is broken so as to create an HO_3 fragment (maximum possible RSE) and an HO_n fragment (RSE = 16 kcal/mol), then the BDE will be 48 − 21 − 16 = 11 kcal/mol.

RSEs can also be used to derive bond dissociation energies for breaking a bond in a radical, e.g., HO_2−O → HO_2 + O. Thus, BDE(HO_2−O)ABE(O−O) − RSE(HO_2) + RSE(HO_3) = 48.69 − 15.42 + 21.16 = 54.43 kcal/mol, and similarly for the other possible radicals.

Table 7. Dissociation Energy (kcal/mol) at 0 K for Hydrogen Polyoxides and Related Fragments

species	G2(MP2)	additivity[a]	exptl	ref
H−O($^2\Pi$)	101.90		101.3	30
HO−H	118.67			
HO_2−H	87.07	87.11	88 ± 1	*c*
HO_3−H	81.29	81.37		
HO_4−H	85.45	85.93		
HO−O(^{2}A″)	64.75	64.72	65.5 ± 0.5	*c*
HO_2−O(^{2}A″)	54.41	54.43	46 ± 2	*c*
HO−O_2 (^{2}A″)	3.45			
HO_2−O_2	−16.94			
HO−OH	49.91	49.91[b]	51 ± 1	*d*
HO_2−OH	33.91	33.88	31.7 ± 1.4	*c*
HO_2−O_2H	17.80	17.85	18	*c*
HO_3−O_2H	12.3 ± 0.3	12.11		
HO_3−OH	27.96	28.14		
HO_4−OH	32.9 ± 0.3	32.70		
HO_2−O_4H	16.46 ± 0.3	16.67		
HO_3−O_3H		6.37		
HO_4−O_3H		10.93		
HO_4−O_4H		15.49		
O_2($^3\Sigma_g^-$)	115.88		118	30
O_2($^1\Delta_g$)	89.25		95	30

[a] For explanation, see text. [b] The additivity scheme uses the G2(MP2) value of 49.91 kcal/mol for BDE as a reference value. The radical stabilization energy of OH is defined so as to give this BDE exactly. [c] Shum, L. G. S.; Benson, S. W. J. Phys. Chem. **1983**, 87, 3479. [d] McMillen, D.; Golden, D. M. Ann. Rev. Phys. Chem. **1982**, 33, 493. [e] From RRKM fit to experimental data.

Table 7 gives the bond dissociation energy (BDE) at 0 K, taken as the difference in the G2 energy (at 0 K) between radical fragments and the parent hydrogen polyoxide, i.e., by using differences between the atomization energies from Table 5 (or E_0 data from Table 4). Alternatively, an additivity scheme can be used where BDE(HO_i−O_jH) = ABE(O−O) − RSE(HO_i) − RSE(HO_j). This is also given in Table 7, for comparison. The G2(MP2) results show relatively good agreement with experimental values for the parent hydrogen polyoxides, where available, with errors lying within about 1 kcal/mol. The HO−O BDE is also calculated to within this accuracy. The HO_2−O BDE appears to have significant error; however, due to the difficulty of obtaining the experimental value and the consis-

(34) Tanaka, T.; Morino, Y. *J. Mol. Spectrosc.* **1970**, *33*, 538.
(35) Herzberg, G. *Electronic Spectra and Electronic Structure of Polyatomic Molecules*; Van Nostrand: New York, 1966.
(36) Leroy, C.; Peeters, D.; Wilante, C. *THEOCHEM* **1982**, *5*, 217.
(37) Sanderson, R. T. *J. Org. Chem.* **1982**, *47*, 3835.

tency of the theoretical results, it seems probable that the experimental value is in error.

For the neutral species, the only results which are poor are those for diatomic oxygen, especially in the singlet state (almost 6 kcal/mol error). These errors have been noted previously by the authors of the G2 methodology.[25] Certainly part of the error is due to the poor bond distances (Table 1) found using the G2(MP2) method for oxygen bond distances. As will be seen in a later section, the error in the estimate of the BDE of singlet oxygen will show up as an error in determination of the reaction barrier along decomposition pathways which produce singlet oxygen.

By comparison of the G2(MP2) BDEs and those derived from the assumption of additivity (constant O−O bond energy + RSEs), we see that the agreement is excellent between the two methods, with deviations generally less than 0.5 kcal/mol. This allows us to extend the calculation of BDE to H_2O_6 or even longer hydrogen polyoxides.

From Table 7 it can be seen that the weakest bond is always in the center of the chain and that the BDE decreases as the chain length increases, going from 49.9 to 33.9, 17.8, 12.3, and 6.4 (estimated) kcal/mol, for H_2O_2, H_2O_3, H_2O_4, H_2O_5, and H_2O_6, respectively. Use of the additivity scheme for RSE to obtain the BDE for H_2O_7 and H_2O_8 would give BDEs of 10.9 and 15.5 kcal/mol, respectively. It is therefore clear from Table 7, and from the discussion of RSE given previously, that the bond dissociation energy of the hydrogen polyoxide chains remains finite (although very small), reaching a minimum value for H_2O_6. Any further increases in chain length will cause the BDE to increase. The answer to "How long can you make an oxygen chain?" is therefore "Infinite in the gas phase, although the temperature of the experiment must be very low since the chain is bound by a very weak link." The chain is weakest for H_2O_6, reaching a minimum (gas-phase) value of about 6 kcal/mol. In solution or even in the solid phase, other modes of decomposition of H_2O_n must be considered, including acid, base, and neutral water catalysis.

Decomposition Pathways

Decomposition pathways for the hydrogen polyoxides have been studied for two decades or more, especially by Plesničar and co-workers. Current understanding as of 1992 was reviewed by Plesničar.[13] There are several points which must be considered in establishing any theoretical reaction path. The first is that the experimental activation energy for decomposition is low, only about 14 kcal/mol.[13,38,] The second is that singlet oxygen, i.e., $^1\Delta_g$, has been observed experimentally in the decomposition products of hydrogen trioxide.[2,13,39]

Nangia and Benson[38] suggested a radical chain mechanism for the decomposition of hydrogen trioxide. On the basis of this mechanism, these authors derived a rate law which was $^3/_2$ order in H_2O_3 concentration. They considered this to be consistent with the experimental data reported by Giguere et al.[1] This chain reaction mechanism will have an activation energy less than that occurring in the initial bond breaking (31.7 kcal/mol, Table 7) and might be considered as a probable path for H_2O_3 decomposition, unless ruled out on other grounds. However, if the propagation steps occur by hydrogen abstraction, they would give $HO_3^\bullet$ as an intermediate. $HO_3^\bullet$ has a BDE of only 3 kcal/mol (Table 7), so this would be followed by fast decomposition to ground-state $HO^\bullet + O_2$ and no singlet oxygen would be observed.

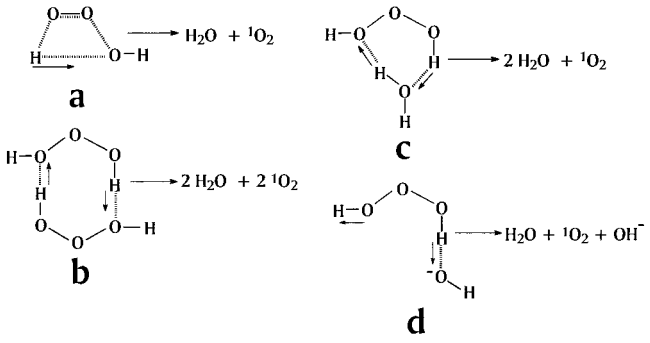

Figure 4. Decomposition pathways for H_2O_3: (a) intramolecular proton transfer; (b) double proton transfer via cyclic dimer; (c) solvent-catalyzed proton transfer; (d) base-catalyzed proton transfer.

Plesničar et al.[40] reported that hydrotrioxides are formed during the ozonation of organic compounds and considered that the most likely decomposition path was the scission of the RO−OOH bond and the subsequent formation of caged radical pairs (i.e., the Benson mechanism, with solvent trapping of radicals). However, attempts to trap the alkyltrioxyl radicals were unsuccessful, and later studies looked for other decomposition pathways.

Plesničar et al.[2] then observed H_2O_3 in decomposition reactions of dimethylphenylsilyl hydrotrioxides. The hydrotrioxides decomposed with evolution of singlet oxygen products. These authors proposed polar pathways involving either (i) an intramolecular transfer of one proton to the most distant oxygen atom, to yield $^1O_2$ and H_2O, or (ii) proton transfer from one H_2O_3 to another H_2O_3, via a cyclic dimer (double proton transfer path). Schematic drawings of these reaction paths are shown in Figure 4a,b.

They carried out an ab initio study of these mechanisms using an RHF/6-31G(d) geometry optimization and RHF/6-31G(d,p) single point energy calculations. They found binding energies in cyclic H_2O_3 dimers of 7−8 kcal/mol but did not report barrier heights in that work. At the same time, Gonzalez et al.[41] began a study of the reaction of OH and HO_2 taking place on a singlet potential surface. This reaction can, in principle, lead to formation of H_2O_3. They found a barrier height of 48.6 kcal/mol using MP2 methods, effectively ruling out this mechanism for the decomposition of H_2O_3.

In another study Plesničar and co-workers formed hydrogen trioxide by the low-temperature ozonation of 2-ethyl anthrahydroquinone.[3] They confirmed, with the use of MP4 calculations, that the transition state for the intramolecular proton-transfer path was ca. 50 kcal/mol above the ground state, i.e., far too high for the reaction to proceed on the singlet surface. On this basis they preferred the dimeric proton-transfer path. They also pointed out in this study, however, that assistance by water acting as a bifunctional (acid/base) catalyst could not be ruled out. A hypothetical transition-state geometry with this structure is shown in Figure 4c. The bifunctional nature of the catalyst is due to its ability to both accept and donate a proton, hence the label proton donor/acceptor pathway on the figure. Plesničar suggested in this work that another conceivable path could involve formation of the base HO_3^-, e.g., as in $H_2O + H_2O_3 \rightarrow HO_3^- + H_3O+$, although they ruled this out on the basis that

(38) Nangia, J. P. S.; Benson, S. *J. Phys. Chem.* **1979**, *83*, 1138; **1980**, *102*, 3105.

(39) Corey, E. J.; Mehrotra, M. M.; Khan, A. U. *J. Am. Chem. Soc.* **1986**, *108*, 2472.

(40) Kovac, F.; Plesničar, B. *J. Am. Chem. Soc.* **1979**, *101*, 2677. Plesničar, B.; Kovac, F.; Schara, M. *J. Am. Chem. Soc.* **1988**, *110*, 214.

(41) , Gonzalez, C.; Theisen, J.; Zhu, L.; Schlegel, H. B.; Hase, W. L.; Kaiser, E. W. *J. Phys. Chem.* **1991**, *95*, 6874; **1992**, *96*, 1767.

Table 8. Transition State Structure for $H_2O_3 + H_2O \rightarrow$ [Transition State] $\rightarrow 2H_2O + {}^1O_2$

distance (Å)	RHF/6-31G(d,p)	MP2/6-31G(d,p)	MP2/6-31++G(d)[a]
O1−O2	1.466	1.835	1.850
O1−H4	0.952	0.975	0.985
O1−H7	1.133	1.336	1.402
O2−O3	1.377	1.297	1.298
O3−H5	1.512	1.305	1.362
O6−H5	1.019	1.140	1.130
O6-O7	1.258	1.117	1.102
O6−H8	0.945	0.967	0.978
$\Delta E_0°$ [b]	47.1	22.8	26.0

[a] Reference 9. [b] Relative to H-bonded reactants $H_2O_3 \cdot H_2O$, in kcal/mol.

strong oxygen bases retard (rather than accelerate) the decomposition of of the hydrogen polyoxides.[3]

Very recently Koller and Plesničar[42] reconsidered the participation of H_2O in the decomposition of H_2O_3. They used MP4//MP2/6-31++G(d) calculations to follow several possible decomposition paths. In this work they found a barrier of 49 kcal/mol for the unassisted intramolecular proton transfer, i.e., for $H_2O_3 \rightarrow H_2O + O_2$ ($^1\Delta_g$). However, they obtained an energy barrier of only 15 kcal/mol (relative to isolated reactants) or 26 kcal/mol (relative to hydrogen bonded $H_2O_3 \cdots H_2O$) for the water-assisted intramolecular 1,3-proton transfer to form water + singlet oxygen. The authors expect that the true barrier will be lowered further if more solvent (water) participates in the decomposition; hence, they have identified a very low-barrier pathway and ruled out some of the alternatives. Furthermore, population analysis showed that the migrating hydrogen behaved as a proton, accumulating significant positive charge during the transfer step. Thus, "proton transfer" as opposed to "hydrogen transfer" is appropriate terminology. This corresponds to the water-assisted decomposition path shown in Figure 4c.

Our own work on H_2O_3 decomposition pathways was completed prior to publication of the Plesničar[42] results, and we verified independently that the isolated intramolecular proton-transfer path had a high barrier (Figure 4a). This led us to consider alternatives such as the unimolecular decomposition of protonated H_2O_3 and eventually to solvent-assisted decomposition paths. For the decomposition of H_2O_3, we considered a hydrogen-bonded water−H_2O_3 complex. Starting from the complex, the transition-state geometry was located using the synchronous transit-guided quasi-Newton method[21] at the MP2/6-31G(d,p) level. The energy of the transition state was then determined using a number of different levels of theory, to get an estimate of the sensitivity of barrier height with respect to level of theoretical treatment.

Bond distances for the transition state structure are shown in Table 8 for both RHF and MP2 calculations, along with the calculations of Plesničar[42] for comparison. The two calculations are slightly different in the choice of basis: our 6-31G(d,p) basis uses p functions on hydrogen, whereas his 6-31++G(d) basis uses diffuse functions on both hydrogen and oxygen.

As can be seen in Table 8, our RHF and MP2 calculations differ substantially in their description, particularly of the oxygen−oxygen bonds and in the position of the bridging hydrogen atoms. In fact, the two descriptions are so different that the RHF calculations cannot even be used to help in a preliminary search for the location of the transition state. Both MP2 calculations are very similar, however, and our work confirms the structure reported by Plesničar.[42] In particular, the very long O1−O2 bond and the very short O2−O3 bond

(42) Koller, J.; Plesničar, B. *J. Am. Chem. Soc.* **1996**, *118*, 2470.

Table 9. Energy Difference $\Delta E_0°$ between O_2 ($^1\Delta_g$) and O_2 ($^3\Sigma_g^-$) (in kcal.mol)[a]

method	calcd	diff
MP2/6-31G(d)	31.00	8.50
MP2/6-311G(d)	30.75	8.25
MP2/6-311+G(3df)	29.17	6.67
QCIST(T)/6-311G(d,p)	30.87	8.37
exptl[b] (ref 30)	22.50	0.00

[a] All theoretical geometries optimized at the MP2/6-31G(d,p) level. [b] Taken as T_e + ZPE($^1\Delta_g$) − ZPE($^3\Sigma_g^-$).

Table 10. Corrected and Uncorrected Energies $\Delta E_0°$ (at 0 K) for $H_2O_3 + H_2O$ Transition State and Products (in kcal/mol) with Hydrogen-Bonded Reactant Energy Set to 0.0 in Each Case[a]

method	TS	TS (corr)	products	products (corr)
MP2/6-31G(d,p)	22.8	14.3	−8.0	−16.5
MP2/6-311G(d,p)	23.3	15.0	−11.4	−19.7
MP2/6-311G(3df,2p)	23.2	16.5	−10.2	−16.9
QCISD(T)/6-311G(d,p)	25.3	16.9	−5.6	−14.0
MP4/6-31++G(d)[b]	23.4		−2.8	

[a] ZPE corrections calculated using (unscaled) MP2/6-31G(d,p) energies. [b] From ref 9.

means that the system has essentially achieved its final $^1O_2$ geometry while still at the transition state. It is therefore important to look at the error introduced in the calculation of singlet oxygen using the various methods A,B,C, etc.

Table 9 shows the energy difference $\Delta E°_0$ between singlet and triplet forms of diatomic oxygen. There is a very substantial overestimate of the triplet−singlet splitting by all methods, ranging from 6.67 to 8.50 kcal/mol. This should therefore be applied as a correction factor to obtain transition-state and product energies relative to the hydrogen-bonded reactants $H_2O_3 + H_2O$.

Table 10 gives the energy difference $\Delta E°_0$ at 0 K for transition state and products, relative to hydrogen-bonded reactants. Data are also given for the corrected transition state energies according to the singlet−triplet overestimates reported in Table 9. The different methods give rather good agreement, with barrier heights ranging from 23 to 25 kcal/mol when uncorrected for singlet−triplet error, or with the correction factor included ranging from 14 to 17 kcal/mol. Since the products are $2H_2O + {}^1O_2$, the correction also applies to products. The energy released at 0 K then ranges from 14 to 20 kcal/mol. These calculations are not yet converged with respect to basis set/correlation treatment, but the results are strongly suggestive that there is a barrier height of ca. 17 kcal/mol relative to hydrogen-bonded reactants. Since in the solid state reported below −50 °C, where it is supposed that water, hydrogen peroxide, and hydrogen trioxide are frozen into a glassy matrix, it seems that the most reasonable form of hydrogen trioxide would be in a hydrogen-bonded solid. In that case, the hydrogen-bonded reactant is the proper choice to establish a reference state, and an experimental activation energy of 14 ± 2.5 kcal/mol[13] is consistent with these calculations.

For bases which are stronger than H_2O, e.g. $(CH_3)_2O$, Plesničar[42] observed that they slow the reaction. This is possible since the base ties up one hydrogen atom in H_2O_3 in a strongly hydrogen-bonded complex, but is unable to donate a hydrogen atom (proton) at the other end, so that a solvent-assisted proton transfer is impossible.

Figure 4d shows another possible path, the base-catalyzed reaction path. To test this path we brought OH^- near H_2O_3, looking for a transition state. Instead, the system fell smoothly into hydrogen-bonded products $H_2O \cdots HO_3^-$ with all positive

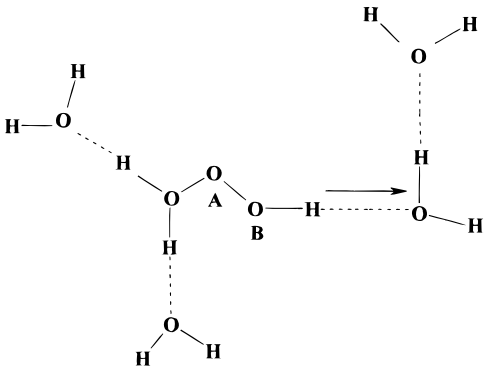

Figure 5. Acid-catalyzed proton transfer decomposition path fopr H_2O_3.

frequencies, i.e., a proton transfer occurred from hydrogen trioxide to hydroxide ion without any barrier. Sufficient data were given by Plesničar[42] to determine that that this outcome is reasonable. The gas-phase ionization of hydrogen trioxide to give $HO_3^- + H^+$ is endothermic by 352 kcal/mol. The gas-phase ionization of water to give $HO^- + H^+$, for comparison, is 391 kcal/mol. Thus the reaction of $HO^- + H_2O_3 \rightarrow H_2O + HO_3^-$ is exothermic by 39 kcal/mol. HO_3^-, in turn, can decompose into singlet oxygen + OH^-, a reaction which is endothermic by 32.5 kcal/mol (all calculations at the MP4 level). The overall result is that $H_2O_3 + HO^- \rightarrow {}^1O_2 + H_2O + HO^-$ is exothermic by 6.5 kcal/mol. Furthermore, it can take place without activation energy, since the initial proton transfer has no barrier, and the decompostion of HO_3^- simply corresponds to dissociation of the weak O−O bond, a process which also has no barrier.[43] In other words, when a very strong base is present (e.g., HO^-), decomposition of hydrogen trioxide will be very rapid without any additional solvent assistance. The complete reaction scheme is then $HO^- + H_2O_3 \rightarrow H_2O + HO_3^-$, followed by $HO_3^- \rightarrow HO^- + {}^1O_2$. For H_2O_4, this base-induced path is also expected to be a low-energy path, since $H_2O_4 + OH^- \rightarrow H_2O + HO_4^-$, followed by rapid decomposition of HO_4^-.

All of the above thermochemistry has been derived from Plesnicar's thermochemical data based on isolated species. In the glassy solid state, as OH^- is in contact with H_2O_3 it will form the HO_3^- anion without a barrier. However, the exothermicity of the reaction will be lost into the solid and will not be available for decomposition. At that point, HO_3^- will be complexed with H_2O, lowering its total energy. The products $OH^- + H_2O$ will also be complexed, lowering their energy as well. The energy difference will probably remain close to the 32 kcal/mol derived for the gas phase. The base-catalyzed path should therefore not be a major contributor to decomposition.

A final path to reaction involves acid catalysis, Figure 5. The overall reaction involving acid catalysis involves conversion of H_2O_3 into $H_2O + {}^1O_2$, but the involvement of acid (H_3O^+) and the number and location of solvent (H_2O) molecules strongly influences the path. This is basically due to the stabilization of the proton by multiple solvent molecules, which delocalizes the positive charge thus reducing the total energy. In the lowest energy path we explored, one molecule of acid and three molecules of solvent were used. The true solvent-assisted path may lie lower in energy but our calculated path will already be shown to have a very low barrier.

The reactants were brought together along the path shown in Figure 5. In this path a reactant minimum is formed corresponding to a protonated H_2O_3 solvated by two water molecules on the left and two on the right. Once the reactant minimum was found, the overall reaction produces $(H_2O)_3 + O_2\ (^1\Delta) + H_3O^+\cdots H_2O$, where the three water molecules form a hydrogen bonded complex as does the $H_3O^+\cdots H_2O$ group.

Because of the tremendous number of degrees of freedom to search and the looseness of the transition state, it was impractical to carry out vibrational frequency calculations and indeed even to exactly locate the true transition state. However, we can nevertheless state the following: Overall, the reaction is exothermic by 15.5 kcal/mol in electronic energy (MP4(full)/6-31G(d) level). Using the bond length O_B-H (Figure 5) as a reaction coordinate and varying only oxygen atom O_A, i.e., along a partially relaxed path, the electronic energy did not go above 6 kcal/mol relative to (complexed) reactants. Allowing for the ZPE correction which will reduce the activation energy, and also the error inherent in the calculation of O_2 ($^1\Delta$) which will act in the same direction, we can say with confidence that the transition state along the acid-catalyzed path will not lie more than 6 kcal/mol above reactants, and probably less. Further improvement on this estimate will be technically difficult since transition-state-searching algorithms have great difficulty when multiple solvent molecules are involved, but the above arguments should be sufficient to demonstrate that when acid catalysis in water is possible, the hydrogen polyoxides will become very unstable.

In the perfluoroalkylated trioxide, $(CF_3)OOO(CF_3)$, neither the solvent-assisted nor the acid- or base-catalyzed paths are possible. Dissociation would then most likely occur along a radical decomposition path, including a chain reaction mechanism. The O−O BDE in the comparable perfluoroalkylated trioxide is ca. 30 kcal/mol which is slightly less than in hydrogen trioxide. This means that the activation energy may still be well in excess of the 14 kcal/mol observed for hydrogen trioxide. This is in agreement with the experimental observation that the perfluoroalkylated trioxide is much more stable than hydrogen trioxide, not decomposing until at or above 25 °C.[5]

Conclusions

Structures of the hydrogen polyoxides have been accurately computed using G2(MP2) theory. Contrary to intuition, the longer polyoxides have bond lengths shorter than those in hydrogen peroxide. The structures can be understood and correctly predicted, including the lowest-energy conformation, by simple hyperconjugation arguments. Thermochemistry is accurately determined (where comparisons are possible) using G2(MP2) theory, and by an extension of the G2(MP2) energy, the radical stabilization energy (RSE) is defined and used to predict the properties of very long chains. This allowed us to answer the title question, "How long can you make an oxygen chain?" by noting that a minimum BDE of 6.4 kcal/mol occurs for the central bond in H_2O_6. Again contrary to intuition, for longer chains the BDE begins will increase above this minimum value.

These results have been used to interpret the known chemistry of the hydrogen polyoxides. Proton-transfer paths are shown to be important in explaining the high reactivity of the polyoxides H_2O_n, where $n > 2$. If these paths can be blocked, as in the fluorinated or perfluoroalkylated polyoxides, then the stability is expected to increase, in agreement with experimental observations.

Acknowledgment. We thank the Natural Sciences and Engineering Research Council of Canada (NSERC) for financial support for this work.

JA971534B